Nuclear fragmentation and its parallels

K. C. Chase and A. Z. Mekjian
Department of Physics, Rutgers University, Piscataway, New Jersey 08854
(Received 13 September 1993)

A model for the fragmentation of a nucleus is discussed. A general framework for obtaining the canonical ensemble partition function for a fragmentation process is developed based on simple recursive techniques. Parallels of the description of this process with other areas are shown which include Feynman's theory of the λ transition in liquid helium, Bose condensation, and Markov process models. These parallels are used to generalize and further develop a previous exactly solvable model of nuclear fragmentation. A comparison with other models is also given and one of these models is generalized to include a tuning parameter which contains the underlying physical quantities associated with the fragmentation process. A discussion of the behavior of the partition function and phase transitions is given in terms of Lee-Yang zeros of the partition function. An analysis of some experimental data is given.

PACS number(s): 25.70.Pq, 05.30.Ch

I. INTRODUCTION

The behavior of the distribution of fragments in an intermediate energy nuclear collision has attracted a great deal of interest [1–20]. A previous set of papers [1–3] proposed a statistical model for describing this behavior. Each possible fragmentation outcome is given a particular probability, and the resulting partition functions and ensemble averages are known to be exactly solvable. In this paper we extend that canonical ensemble model to allow more freedom in choosing the weight associated with a particular nuclear partition. Formulas for the ensemble averages and the partition function derived in earlier papers are generalized, and a recursive formula for the evaluation of the coefficients of the partition function is developed which is useful in computing low and high temperature behavior of the models. This paper also focuses on a more detailed discussion of the properties of these partition functions than the previous papers.

The balance of the paper is concerned with the application of these results to models of nuclear fragmentation, as well as a comparison of these results both to other models in physics and to other models of fragmentation. An explicit parallel between this model and Feynman's approach [21] to the λ transition in liquid helium is proposed. The weight given to each possible cluster distribution in a canonical ensemble model is shown to be similar to that used by Feynman in the cycle class decomposition of the symmetric group. Moreover, the main parameter, called the tuning parameter x in Ref. [1], which contains the physical quantities associated with cluster formation, is shown to have a correspondence with a variable in Feynman's approach related to the cost function of moving a helium atom from one location to another. The variable associated with this cost function is related to that part of the parameter x which has to do with internal excitations in a cluster, i.e., its internal partition function.

Other models of fragmentation are easily compared to the canonical ensemble model. Models based on partitioning alone [4,5] are discussed briefly. They are also a result of assuming a certain weight is associated with each nuclear fragmentation outcome. However, the choice of weight is simpler than the models proposed here. These models are also generalized in this paper to include a tuning parameter which contains the underlying physical quantities associated with the fragmentation process. Models based on percolation studies [6,7] also have some similar features. Markov process models [22] are not only similar to canonical ensemble models, but rather are the exact same models, simply derived from a different, phenomenological, point of view. This is fortuitous, as an analogy with Markov process models can provide the basis for choosing particular canonical ensemble models for the study of nuclear fragmentation. A final model of fragmentation to compare the canonical ensemble model with is a further generalized iterative canonical ensemble models, of which canonical models are a special case. Canonical models have many advantages over this proposed generalization, but such generalized models may be useful in studying exotic fragmentation situations.

A section of this paper is devoted to the discussion of the thermodynamic functions of canonical ensemble models. Since the canonical models are derived from a statistical mechanics assumption, it is appropriate to consider the computation of the typical thermodynamic functions. After deriving the appropriate formulas, they are applied to the case of an ideal Bose gas in d dimensions as an illustration. The critical point, present for $d > 2$, is discovered by plotting the specific heat vs the temperature. The connection between the Lee-Yang zeros of the partition function and the critical behavior is also considered, as the recursion relations allow for the computation of the zeros for some nontrivial cases. The zeros for $d = 2$ and $d = 4$ are computed, and empirically appear to lie on simple arclike curves. This behavior is compared with the distribution of zeros of the Ising model.

A set of extended canonical models, suggested by the analogies to other models, are applied to the experimen-

tally determined nuclear fragmentation distribution. After reviewing the general behavior of a number of models, which are found to vary widely in their fragmentation behavior, we focus on a small number of models which seem to be appropriate for an ensemble description of the fragmentation of $^{197}_{79}$Au at 0.99 GeV/nucleon. Several models give excellent results, but the statistics of the experimental data are not sufficient to distinguish a particular model from the others considered. One particular model, although a poor model of nuclear fragmentation, has very interesting properties and is analyzed further. In this model, the fragmentation process favors fragments of a particular size, with a Gaussian falloff in the distribution for larger and smaller fragments. For example, for particular choices of the tuning parameter, the fragment distribution will be that of a system that has split into two equally sized pieces.

The paper is organized as follows. Section II develops the canonical model for fragmentation and briefly discusses parallels of this model with the λ transition in liquid helium and Bose condensation. Section III discusses a variety of other models for the fragmentation of a nucleus. Alternative partitioning models and percolation models are reviewed briefly. Markov process models and generalized canonical models are introduced. The thermodynamic properties of fragmentation models, including the calculation of thermodynamic functions and the determination of phase transitions from the zeros of the partition function, are considered briefly in Sec. IV. Section V discusses the behavior of the ensemble averages for various models and compares these models with some experimental data. Concluding remarks are made in Sec. VI.

II. MODELS OF FRAGMENTATION AND PARTITIONING PHENOMENA

In this section, we review an approach to fragmentation and partitioning phenomena based on the canonical ensemble of statistical mechanics. In this approach the fragmentation of a nucleus, or, in general, an object, is viewed in a statistical way with a weight given to each member in the ensemble of all possible distributions. Mean quantities, correlations, and fluctuations are obtained by averaging various expressions over the ensemble using this weight. The model considered is not limited to descriptions of nuclear fragmentation, and the rest of this section is devoted to introducing other areas in physics which have used a similar type of description. Specifically, Feynman's description of the λ transition in liquid helium and Bose condensation are discussed.

A. Exactly solvable canonical models

Exactly solvable canonical models, which can be used for the study of fragmentation and partitioning phenomena, were developed in a previous set of papers [1–3]. Each partition or fragmentation is given the weight

$$P_A(\mathbf{n},\mathbf{x}) = \frac{A!}{Q_A(\mathbf{x})}\prod_{k=1}^{A}\frac{1}{n_k!}\left(\frac{x_k}{k}\right)^{n_k} \tag{1}$$

where $\mathbf{n} = (n_1,\ldots,n_A)$ is the partition vector for the fragmentation or partitioning of the A objects into n_k clusters of size k, and $\mathbf{x} = (x_1,\ldots,x_A)$ is the parameter vector with x_k characterizing the group or cluster of size k. The partition vector must satisfy the constraint $\sum_{k=1}^{A} kn_k = A$ and we denote the set of all partition vectors Π_A. The parameter vector contains the underlying physical quantities such as the temperature T and the volume V. The probability condition for $P_A(\mathbf{n},\mathbf{x})$

$$\sum_{\mathbf{n}\in\Pi_A} P_A(\mathbf{n},\mathbf{x}) = 1 \tag{2}$$

determines the partition function $Q_A(\mathbf{x})$ when Eq. (1) is substituted into Eq. (2).

Previous papers dealt with two particular models in detail. When all the $x_k = x$, the x model of Ref. [1], the partition function takes on a simple form

$$Q_A(x) = x(x+1)\cdots(x+A-1) = \frac{\Gamma(x+A)}{\Gamma(x)}\,. \tag{3}$$

For the case $x_1 = xy, x_k = x, k \neq 1$, the xy model of Ref. [3],

$$Q_A(x) = \sum_{k=1}^{A}\binom{A}{k}\frac{\Gamma(x+k)}{\Gamma(x)}[x(y-1)]^{A-k}\,. \tag{4}$$

Detailed studies [3] show that the results of the x and xy models are quite similar for all cluster sizes $k > 1$.

This paper considers in detail more general forms for x_k. Here, we explicitly show how to evaluate the partition function by simple recursive procedures. For convenience, we rewrite Eq. (1) by making the following substitution

$$x_k(A,V,T) = \frac{kx(A,V,T)}{\beta_k}\,, \tag{5}$$

so that the dependence on the physical quantities is contained within a single parameter x and the thermodynamic dependence and cluster size dependence are separable. Then the weight is given by

$$P_A(\mathbf{n},x,\boldsymbol{\beta}) = \frac{A!}{Q_A(x;\boldsymbol{\beta})}\prod_{k=1}^{A}\frac{1}{n_k!}\left(\frac{x}{\beta_k}\right)^{n_k}\,. \tag{6}$$

This is not an unreasonable constraint on the parameters, and is easily satisfied by many models. For example, a previous paper [1] developed the result

$$x = \frac{V}{v_0(T)}\exp\left\{-\frac{a_\nu}{k_BT} - \frac{k_BT}{\varepsilon_0}\frac{T_0}{T+T_0}\right\},$$
$$\beta_k = k \tag{7}$$

where T is the equilibrium temperature, V is the freeze-out volume, and $v_0(T) = h^3/(2\pi m_p k_B T)^{3/2}$ is the quan-

tum volume, with m_p the mass of a nucleon. The a_ν is the coefficient in a simplified equation for the binding energy of a cluster of size k, $E_B = a_\nu(k-1)$. The ε_0 is the level density parameter related to the spacing of excited levels and T_0 is a cutoff temperature for internal excitations. In a Fermi gas model, ε_0 and the Fermi energy are related by $\varepsilon_0 = 4\varepsilon_F/\pi^2$, and since $\varepsilon_F = p_F^2/2m_p$ can be obtained from $4(4\pi p_F^3 V/3h^3) = A$, we find that

$$\frac{k_B T}{\varepsilon_0} = \left(\frac{\pi}{12}\right)^{2/3} \frac{2m_p k_B T}{\hbar^2} \left(\frac{V}{A}\right)^{2/3} . \tag{8}$$

The evaluation of the partition function $Z_A(x;\boldsymbol{\beta}) = Q_A(x;\boldsymbol{\beta})/A!$ and the various ensemble averages can be derived from the generating function for $Z_A(x;\boldsymbol{\beta})$. Using this function, it was shown in Ref. [3] that the ensemble averaged cluster distribution $\langle n_k \rangle$ is given by

$$\langle n_k \rangle = \frac{x}{\beta_k} \frac{Z_{A-k}(x,\boldsymbol{\beta})}{Z_A(x,\boldsymbol{\beta})} . \tag{9}$$

where $Z_k(x;\boldsymbol{\beta}) = 0$ for $k < 0$. More generally, it was shown that

$$\left\langle \prod_{k=1}^{A} [n_k]_{p_k} \right\rangle = \left\{ \prod_{k=1}^{A} \left(\frac{x}{\beta_k}\right)^{p_k} \right\} \frac{Z_{A-\sum k p_k}(x;\boldsymbol{\beta})}{Z_A(x;\boldsymbol{\beta})} \tag{10}$$

where the falling factorial $[z]_k$ is defined by $[z]_k \equiv (z-k+1)[z]_{k-1}$ with $[z]_0 = 1$.

The constraint $\sum_{k=1}^{A} k\langle n_k \rangle = A$ then leads to a simple recurrence relation for $Z_A(x,\boldsymbol{\beta})$:

$$Z_A(x,\boldsymbol{\beta}) = \frac{x}{A} \sum_{k=1}^{A} Z_{A-k}(x,\boldsymbol{\beta}) \frac{k}{\beta_k} \tag{11}$$

with $Z_0(x,\boldsymbol{\beta}) = 1$. Then $Z_1(x,\boldsymbol{\beta}) = x/\beta_1$, and so on. We can now calculate any ensemble average of n_k using Eqs. (9) and (10), once the partition function is obtained from Eq. (11). We therefore turn our attention to a detailed study of the partition function.

From the last equation we see that $Z_A(x,\boldsymbol{\beta})$ is a polynomial in x of order A. To encourage this point of view, we will drop the dependence on $\boldsymbol{\beta}$ from the notation for Z_A, making the dependence tacit. Then, the partition function can be written as

$$Z_A(x) = \sum_{m=1}^{A} Z_A^{(m)} x^m \tag{12}$$

where the coefficients $Z_A^{(m)}$ can be determined from the recurrence relationship as follows. The first coefficient, $Z_A^{(1)}$, is determined by the last term in the recurrence relation, $(x/A)AZ_0(x)/\beta_A = x/\beta_A$. So $Z_A^{(1)} = 1/\beta_A$. From this coefficient we can determine all the others by substituting Eq. (12) into Eq. (11), arriving at

$$Z_A^{(m)} = \frac{1}{A} \sum_{k=1}^{A-m+1} \frac{k}{\beta_k} Z_{A-k}^{(m-1)} . \tag{13}$$

Thus the coefficients $Z_A^{(m)}$ can also be obtained recursively. For m near A, this expression can be used to obtain exact results for the coefficients. Assuming $\beta_1 = 1$, which can always be done by redefining x, β_k such that x/β_k is unchanged (i.e., $x \to x/\beta_1$, $\beta_k \to \beta_k/\beta_1$), we find

$$\begin{aligned}
Z_A^{(A)} &= \frac{1}{A!} , \\
Z_A^{(A-1)} &= \frac{1}{(A-2)!\beta_2} , \\
Z_A^{(A-2)} &= \frac{1}{(A-3)!\beta_3} + \frac{1}{2(A-4)!\beta_2^2} , \\
Z_A^{(A-3)} &= \frac{1}{(A-4)!\beta_4} + \frac{1}{(A-5)!\beta_2\beta_3} + \frac{1}{6(A-6)!\beta_2^3} , \\
Z_A^{(A-4)} &= \frac{1}{(A-5)!\beta_5} + \frac{1}{(A-6)!}\left(\frac{1}{2\beta_3^2} + \frac{1}{\beta_2\beta_4}\right) \\
&\quad + \frac{1}{2(A-7)!\beta_2^2\beta_3} + \frac{1}{24(A-8)!\beta_2^4} .
\end{aligned} \tag{14}$$

In general $Z_A^{(A-m)}$ depends on $\beta_2, \ldots, \beta_{m+1}$ for $m < A/2$.

The recurrence relation given by Eq. (11) is simply solved for the case $\beta_k = k$ (as previously noted) which gives

$$Z_A(x;\beta_k = k) = \frac{1}{A!} \sum_k |S_A^{(k)}| x^k \tag{15}$$

where $S_A^{(k)}$ are Stirling numbers of the first kind. This model was analyzed extensively in Refs. [1–3].

Another case which reduces to a simple polynomial is $\beta_k = 1$ which gives

$$Z_A(x;\beta_k = 1) = \frac{1}{A} x L_{A-1}^1(-x) \tag{16}$$

with $L_A^1(x)$ a Laguerre polynomial. The $\beta_k = 1$ model is considered in detail in [12] as a model for fragmentation and in [22] as an example of a Markov process model for clusterization of one dimensional objects.

A final example whose coefficients are common mathematical functions is $\beta_k = k!$,

$$Z_A(x;\beta_k = k!) = \frac{1}{A!} \sum_{k=1}^{A} \mathcal{S}_A^{(k)} x^k \tag{17}$$

with $\mathcal{S}_A^{(k)}$ Stirling numbers of the second kind. This choice for the case $x = 1$ was considered in detail in Ref. [10]. It will also be analyzed more generally in Sec. V A.

For any choice of β_k, the recursion relation given in Eq. (11) holds. However, for some β_k there are simpler recursion relations. For example, if $Q_A(x)$ is given by an orthogonal polynomial (e.g. $\beta_k = 1$), then $Q_{A+1}(x) = (a_A + b_A x)Q_A(x) - c_A Q_{A-1}(x)$, as given in Abramowitz and Stegun [23]. Table I lists some of these models. Note that the last choice for β_k in Table I can be related to the Catalan numbers, $C_k = \frac{1}{k+1}\binom{2k}{k}$. Specifically, $\beta_k = 2^{2(k-1)}/C_{k-1}$.

All the cases considered so far are special cases of some

TABLE I. Recursion relations for various β_k.

β_k	Recursion relation
k	$Q_{A+1} = (x + A)Q_A$
$k!$	$Q_{A+1} = (x + x\frac{d}{dx})Q_A$
1	$Q_{A+1} = (x + 2A)Q_A - A(A-1)Q_{A-1}$
$2^{2(k-1)}k\binom{2(k-1)}{k-1}^{-1}$	$Q_{A+1} = \frac{1}{2}(2A-1)Q_A + x^2 Q_{A-1}$

general forms. The cases $\beta_k = 1, k, 2^{2(k-1)}/C_{k-1}$ can be realized from

$$\beta_k = \frac{k![c]^{k-1}}{[a]^{k-1}[d]^{k-1}} \tag{18}$$

where the rising factorial $[z]^k$ is defined by $[z]^k \equiv (z + k - 1)[z]^{k-1}$ with $[z]^0 = 1$. For example, the choice $\beta_k = 2^{2(k-1)}/C_{k-1}$ is given by $a = \frac{1}{2}$, $c = d$. The case $\beta_k = k!$ is a special case of

$$\beta_k = \frac{k![c]^{k-1}}{[a]^{k-1}} \ . \tag{19}$$

One case which does not reduce to a commonly known polynomial and is of general interest is $\beta_k = k^\tau$ for $\tau > 1$. In the large A limit, the coefficients are given by $Z_A^{(m)} = z_A^{(m)}/\beta_A$ where $z_A^{(m)}$ are only weakly dependent on A for small m. Table II gives the large A limit for the first few coefficients. Notice that $\lim_{A\to\infty} z_A^{(2)} = \zeta(\tau)$.

We further illustrate the recursive approach with some examples. Consider the ideal Boltzmann gas, $Z_A(x) = x^A/A! = (x/A)Z_{A-1}(x)$. This is equivalent to the x model with the choice of parameters

$$\frac{x}{\beta_k} = \frac{V}{v_0(T)}\delta_{k1} \tag{20}$$

Since $x/\beta_k = 0$ for $k \neq 1$, this model only has "fragments" of size 1, i.e., there is no clusterization.

Another example is given by the Mayer cluster expansion for an ideal Bose gas in d dimensions. In this case the partition function is given by the x model with the choice

$$x = \frac{V}{v_0(T)} \ ,$$
$$\beta_k = k^{1+d/2} \ . \tag{21}$$

This choice with x given by Eq. (7) could also be used as a model for fragmentation, suggesting a parallel between fragmentation and Bose condensation. In Bose systems, however, the "clusterization" occurs in momentum space, not in real space. For example, the formation of the large $k = A$ cluster in a fragmentation process has its analog in the Bose condensation into the ground state in momentum space.

TABLE II. Values of $z_A^{(k)}$ in the large A limit.

τ	$z_A^{(1)}$	$z_A^{(2)}$	$z_A^{(3)}$	$z_A^{(4)}$	$z_A^{(5)}$
3/2	1.000	2.612	3.412	2.971	1.941
2	1.000	1.645	1.353	0.742	0.305
5/2	1.000	1.342	0.899	0.402	0.135
3	1.000	1.202	0.723	0.289	0.0870

One other example of a recurrence relation in statistical mechanics is the interacting Boltzmann gas. For this example, Feynman [21] showed that when the three body and higher order terms are neglected, the spatial part of the recurrence relation is given by

$$Z_{A+1}(V,T) = V\left(1 - \frac{a}{V}\right)^A Z_A(V,T) \tag{22}$$

where $Z_0(V,T) = 1$, $a = \int_0^\infty \left(1 - e^{-V(r)/k_BT}\right) 4\pi r^2 dr$, and $V(r)$ is the two-body potential.

We now briefly discuss some applications to other physical systems and illustrate the parallel with fragmentation phenomenon.

B. Parallel with Feynman's approach to the λ transition in liquid helium

In this section we give some of the results of Feynman's approach [21] for the λ transition which are relevant for the analogy to be discussed. Further details of the results quoted can be found in [21] and the references therein.

The starting point is the partition function obtained by a path integral, given by Eq. (11.52) in Ref. [21]

$$e^{-F/k_BT} = \frac{1}{N!}\left(\frac{2\pi m' k_B T}{h^2}\right)^{3N/2} \times \sum_{P\in S_N} \int d^3\mathbf{R}_1 \cdots d^3\mathbf{R}_N \rho(\mathbf{R}_1, \ldots, \mathbf{R}_N) \times \exp\left\{-\frac{m' k_B T}{2\hbar^2}\sum_i (\mathbf{R}_i - P(\mathbf{R}_i))^2\right\} \tag{23}$$

where N is the total number of helium atoms, m' is the effective mass, $\mathbf{R}_i$ the coordinate of the ith helium atom, $\rho(\mathbf{R}_1, \ldots, \mathbf{R}_N)$ is the potential contribution, and P is the permutation operator. A given permutation among the particles is illustrated in Fig. 1, and can be visualized as the atoms being connected by a set of edges, the edges forming polygons (cycles) of various sizes (cycle

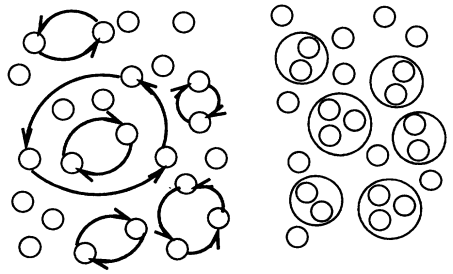

FIG. 1. Permutations among particles. Left-hand side of graph shows a group of particles and a permutation operator as it would act on the particles. Right-hand side gives cluster interpretation of the same permutation.

lengths). After some algebra and approximations, the partition function is reduced to

$$e^{-F/k_BT} = \sum_{\mathbf{n}\in N_N} \prod_{k=1}^{N} \frac{1}{n_k!}\left(\frac{Nh_k}{k}\right)^{n_k} \times \exp\left\{-\frac{m'd^2k_BT}{2\hbar^2}\sum_{k=2}^{N} kn_k\right\} \quad (24)$$

where $h_k = (c/k^{3/2} + 1/N)l^k$, with l the number of nearest neighbors per lattice site for a particular choice of spatial discretization. This result is arrived at by a random walk argument. Specifically, starting at a given atom, there are l^k random walks in k steps, and the fraction of these that are close (end up at the origin) is inversely proportional to the volume in which the random walk is likely to end. This volume is in turn proportional to $k^{3/2}$. The random walk result is then corrected for the very large polygons that encompass a large fraction of the sites. This determines the form for h_k, as given above.

Comparing the results of this section with those of Sec. II A, we see a strong parallel between the model of fragmentation and the model for the λ transition. First, the exponent of Eq. (24) is identical to that internal excitation function of Eqs. (7), and (8), up to a numerical constant, if we neglect the cutoff temperature factor ($T_0 \to \infty$) and make substitutions for the density ($A/V \to d^{-3}$) and the quantum volume [$v_0(T) \to d^3$]. Secondly h_k^{-1} is analogous to the parameter β_k in Eq. (6). In fact, the modification Feynman makes to h_k can be well motivated in the case of nuclear fragmentation, and we will consider the case $1/\beta_k = a/k + (1-a)/k^\tau$ in Sec. V B. Third, the partition function has a formal structure identical to the xy model.

From the above remarks we note two important issues in the choice of weight given to each partition, fragmentation or grouping. One issue is the choice of β_k and the second is the relation of x to the physical quantities.

III. COMPARISON WITH OTHER MODELS OF FRAGMENTATION

In this section, we discuss a number of other models of nuclear fragmentation. Models based on partitioning alone [4,5] are similar to the model outlined in Sec. II A but with a simpler choice for the partition weight. Percolation models [6,7] are derived from far different assumptions. Markov process models are identical to the x model, but derived from a phenomenological point of view. They are useful for considering what forms of β_k would be appropriate for modeling fragmentation phenomenon. Lastly, a generalized canonical model is introduced. Although it does not allow for easy computation of the various ensemble averages, it may be useful in investigating the behavior of exotic partition functions.

A. Models based on partitioning alone

Sobotka and Moretto [4] and Aichelin and Hufner [5] discussed a model of fragmentation based on partitioning alone with no microstate counting factor or tuning parameter. In particular, their assumption is that every partition is equally likely and that alone determines the fragmentation. The number of partitions of A is P_A which can be obtained from the generating function

$$\sum_{A=0}^{\infty} P_A x^A = \prod_{A=1}^{\infty} \frac{1}{1-x^A} . \quad (25)$$

This is asymptotically given by the Hardy-Ramanujan result $P_A \approx e^{\pi\sqrt{2A/3}}/(4A\sqrt{3})$. In this approach the distribution of clusters of size k is given by

$$\langle n_k\rangle = \frac{1}{P_A}\sum_{n=1}^{A} P_{A-nk} \quad (26)$$

which for large A is asymptotic to

$$\langle n_k\rangle \approx \frac{1}{\exp\{(\frac{\pi^2}{6A})^{1/2}k\} - 1} . \quad (27)$$

The above simple model of fragmentation can be generalized to include a tuning parameter x which contains the underlying physical quantities such as volume, temperature, binding, and excitation energy associated with a fragmentation process. In this generalization of the models given in Refs. [4,5], the weight given to any partition is simply x^m which gives the partition function

$$Q_A(x) = \sum_{m=1}^{A} P_A^{(m)} x^m , \quad (28)$$

where $P_A^{(m)}$ is the number of partitions of A with fixed multiplicity $m = \sum_{k=1}^{A} n_k$ and is given by the recurrence relation $P_A^{(m)} = P_{A-1}^{(m-1)} + P_{A-m}^{(m)}$. Once $Q_A(x)$ is obtained, various ensemble averages can be found. For example,

$$\langle n_k\rangle = \frac{1}{Q_A(x)}\sum_{n=1}^{A} x^n Q_{A-nk}(x) . \quad (29)$$

For large A and $xA \gg 1$, $\langle n_k\rangle$ now approaches

$$\langle n_k\rangle \approx \frac{1}{\frac{1}{x}\exp\left\{\left(\frac{\pi^2 x}{6A}\right)^{1/2}k\right\} - 1} . \quad (30)$$

At $x = 1$, the above formula reduces to the result of Eq. (27), as expected.

B. Percolation models

The x model has one variable that describes the degree of fragmentation. As x ranges from 0 to ∞, the temperature changes over the same range. Another one

parameter approach to cluster distributions is based on percolation. The application of percolation to nuclear fragmentation was developed by several groups [6,7]. The percolation models are of two types: bond and site. The bond type assigns a certain probability p of having a bond between lattice sites, while the site type assigns a certain probability of having a site occupied. Similarly, the x of Eq. (7) has terms which deal with volume or density effects, and binding effects. Also included in x are thermal effects through $v_0(T)$ and internal excitation energy considerations which are not present in the percolation models.

In percolation studies, the number of clusters of size k is given by

$$\langle n_k \rangle = \frac{1}{k^\tau} f((p - p_c)k^\sigma) \tag{31}$$

where p_c is the critical probability above which an infinite cluster exists, f is a scaling function, and τ, σ are critical exponents. For the choice $\beta_k = k$, $x = 1 + \epsilon$, with $\epsilon \ll 1$, the x model has a cluster distribution approximately given by (see Ref. [3])

$$\langle n_k \rangle \approx \frac{x}{k} e^{-\epsilon k/A} \tag{32}$$

for $k \ll A$. This is equivalent to a percolation model with x analogous to p, $x_c = 1$, and $f(x) = e^{-x/A}$. This implies the exponents are given by $\sigma = 1$, $\tau = 1$. Other choices for β_k would give a different σ, τ.

C. Markov process models

An alternative point of view for modeling nuclear fragmentation comes from Markov processes, which allows the underlying physical phenomena to be reflected in the equilibrium distributions. The idea is to consider a method by which a cluster configuration can change into another configuration, and then to derive what the equilibrium distribution is for such a method applied to the set of states. Rather than assuming what the probability for each state is, it is derived from the distribution achieved by applying the Markov process repeatedly.

For example, we can consider that the underlying physical processes are the joining of two fragments to form a new larger fragment and the splitting of a larger fragment into two smaller fragments. Fragments joining and breaking into more than two groups are possible, but we will ignore that for now, assuming that those processes are of lesser importance and will not materially affect the overall equilibrium distribution. We denote these processes by a transition operator T which acts as follows on $\mathbf{n}$, the configuration vector.

$$\begin{aligned} T^{jk}\mathbf{n} &= (\ldots, n_j - 1, \ldots, n_k - 1, \ldots, n_{j+k} + 1, \ldots) , \\ T^{jj}\mathbf{n} &= (\ldots, n_j - 2, \ldots, n_{2j} + 1, \ldots) , \\ T_{jk}\mathbf{n} &= (\ldots, n_j + 1, \ldots, n_k + 1, \ldots, n_{j+k} - 1, \ldots) , \\ T_{jj}\mathbf{n} &= (\ldots, n_j + 2, \ldots, n_{2j} - 1, \ldots) . \end{aligned} \tag{33}$$

Suppose these processes occur at some rate, denoted by $q(\mathbf{n}, \mathbf{n}')$ for $\mathbf{n}$ transforms to $\mathbf{n}'$. For example,

$$\begin{aligned} q(\mathbf{n}, T^{jk}\mathbf{n}) &= \lambda_{jk} n_j (n_k - \delta_{jk}), \\ q(\mathbf{n}, T_{jk}\mathbf{n}) &= \mu_{jk} n_{j+k} . \end{aligned} \tag{34}$$

This is a very reasonable choice, as the probability is proportional to the number of fragments available for such moves. If there are none, then the transition probability is zero, as needed. We expect that this process when applied repeatedly to a configuration will lead to an equilibrium configuration, at which point the rate at which transitions occur to a new state, weighed to reflect the equilibrium distribution of the original state, is equal to the rate at which transitions occur back to the original state, weighed to reflect the equilibrium distribution of the new state. In other words, if $P_A(\mathbf{n})$ is the equilibrium distribution, it must satisfy the detailed balance condition:

$$P_A(\mathbf{n}) q(\mathbf{n}, T^{jk}\mathbf{n}) = P_A(T^{jk}\mathbf{n}) q(T^{jk}\mathbf{n}, \mathbf{n}) . \tag{35}$$

If there exist positive numbers $c_1, \ldots, c_A$ such that

$$c_j c_k \lambda_{jk} = c_{j+k} \mu_{jk} \tag{36}$$

then it can be shown that the equilibrium distribution is given by

$$P_A(\mathbf{n}) = \frac{1}{Z_A(\mathbf{c})} \prod_{k=1}^{A} \frac{c_k^{n_k}}{n_k!} . \tag{37}$$

So if for some choice of λ_{jk}, μ_{jk}, we get $c_k \equiv x/\beta_k$, then the models considered in Sec. II A are reproduced. Once we know c_k we can use Eqs. (10) and (11) to solve for the various ensemble averages. In fact, the recursion relationship stated above is another way of expressing the recursion relationship relating partition functions developed in Sec. II A. Of course we still have not produced a set of λ_{jk}, μ_{jk} which satisfy Eq. (36). A very general solution (though not unique) is given by the choice

$$\begin{aligned} \lambda_{jk} &= \alpha f_j f_k , \\ \mu_{jk} &= \beta f_{j+k} \end{aligned} \tag{38}$$

where f_k is any nonnegative function of k. It can be shown that the solution to this model (in the language of the x model) is

$$\begin{aligned} x &= \beta/\alpha , \\ \beta_k &= f_k . \end{aligned} \tag{39}$$

Table III lists some typical examples.

An application of this technique is given by Kelly [22] (Chap. 8). There, Kelly models the polymerization of organic molecules by a Markov process. He assumed

TABLE III. Markov process models.

λ_{jk}	μ_{jk}	x	β_k
α	β	β/α	1
$\alpha(jk)^\tau$	$\beta(j+k)^\tau$	β/α	k^τ
α	$\beta\binom{j+k}{j}^\tau$	β/α	$k!^\tau$

that the molecules combine to form polymers by forming bonds between molecules, up to a maximum of f bonds on a single molecule. If existing bonds between molecules break at a rate κ and new bonds form at a rate proportional to the number of sites available for new bonds, then one can show that the equilibrium polymer distribution is given by applying the x model with $x = \kappa$ and $\beta_k = k![(f-2)k+2]!/[(f-1)k]!$. In this case A is the number of molecules and n_k is the number of polymers containing k molecules.

As an application to the problem of nuclear fragmentation, suppose we think of the fragmentation process as having all the nucleons constrained to move in a small volume of space for a period of time long enough for the fragments to achieve an equilibrium. The probability of joining two fragments should be determined mostly by the density of the nucleons in this volume, and the cross section of each fragment. We expect larger nuclei to accrete smaller nuclei due simply to their larger cross section. Therefore λ_{jk} should increase monotonically in j and k. All the nuclei created can break up into smaller nuclei. We expect larger nuclei to be more unstable than smaller nuclei. This is not strictly correct, as larger nuclei are energetically favorable in their ground state configurations. However, in the aftermath of a high energy collision, the added excitation energy and angular momentum should make larger structures unstable. Therefore μ_{jk} should increase monotonically in j and k as well. This suggests that the above example might be a reasonable model of nuclear fragmentation, provided f_k increases monotonically. A simple choice would be $f_k = \beta_k = k^\tau$ which we will investigate in Sec. V A.

D. Generalized canonical models

As a final example of a model of fragmentation, we discard the notion that the model must be derived from any particular choice of weight. Indeed, the usual process of choosing a weight and then deriving its partition function can be reversed. A partition function can be chosen, and a weight scheme that generates such a partition function can be computed. It is important to note that the choice of a partition function is not sufficient for fixing such a weight scheme. Many different choices for a weight lead to the same partition function and only additional assumptions can fix the weight scheme. For example, the models given by the weight

$$P_A(\mathbf{n},x) = \frac{A!x^m}{Q_A(x)}\prod_{k=1}^{A}\frac{1}{n_k!k^{n_k}} \tag{40}$$

and by the weight

$$P_A(\mathbf{n},x) = \frac{A!x^m}{Q_A(x)}\frac{S_A^{(m)}}{\mathcal{S}_A^{(m)}} \tag{41}$$

where $m = \sum_k n_k$ both give the same partition function $Q_A(x) = x(x+1)\cdots(x+A-1)$. In the first weight, configurations with the same number of fragments have different weights. In the second weight, configurations with the same number of fragments have the same weight.

Suppose that we are given a partition function $Q_A(x) = \sum_{m=1}^{A} Q_A^{(m)}x^m$ where $Q_A^{(m)} \geq 0$ and we want to determine a weight scheme that generates this partition function. For the canonical model with $\beta_k = k$, the weight is given by $W_A(\mathbf{n}) = M_2(\mathbf{n})x^m$, where $m = \sum_k n_k$, $M_2(\mathbf{n}) = A!/\prod_k n_k!k^{n_k}$. An obvious generalization of this weight would be the choice $W_A(\mathbf{n}) = W_A^{(m)}M_2(\mathbf{n})x^m$, i.e., $W_A(\mathbf{n})$ is equal to the standard canonical model weight, up to a factor that depends only on the total number of fragments. For this weight,

$$\sum_{\mathbf{n}\in\Pi_A^{(m)}} W_A(\mathbf{n}) = W_A^{(m)}|S_A^{(m)}|x^m = Q_A^{(m)}x^m \tag{42}$$

where $\Pi_A^{(m)}$ is the set of all partitions of A with multiplicity m, and $S_A^{(m)}$ is the Stirling number of the first kind. This implies that the weight is given by

$$W_A(\mathbf{n}) = \frac{Q_A^{(m)}}{|S_A^{(m)}|}M_2(\mathbf{n})x^m\,. \tag{43}$$

Now if we could write down the generating function for $Q_A(x)$ we could compute $\langle n_k\rangle$ as was done in Sec. II A. However, in general there is no generating function for $Q_A(x)$. We can calculate the expected multiplicity $\langle m\rangle$ using Eq. (52). The $\langle n_k\rangle$ results are not entirely inaccessible. They can be obtained by a Monte Carlo simulation of the weight. Note first that the partition function can be expressed as a sum over the permutation group:

$$\begin{aligned} Q_A(x) &= \sum_{\mathbf{n}\in\Pi_A} M_2(\mathbf{n})\frac{Q_A^{(m)}}{|S_A^{(m)}|}x^m \\ &= \sum_{p\in S_A}\frac{Q_A^{[m(p)]}}{|S_A^{[m(p)]}|}x^{m(p)} = \sum_{p\in S_A} e^{-S(p)} \end{aligned} \tag{44}$$

where $S(p) = \ln|S_A^{[m(p)]}| - \ln Q_A^{[m(p)]} - m(p)\ln x$. We can simulate this action over the set of permutations using the Metropolis algorithm.

One example of a generalized canonical model is given by the partition functions generated by

$$Q_{A+1}(x) = Q_A\left(\frac{ax+b}{cx+d}\right)(cx+d)^{A+1} \tag{45}$$

with $Q_1(x) = x$. Models of this type satisfy a simple recurrence relation, but that recurrence relation is quite different than the canonical recurrence relation given in Eq. (11). Another model, even more exotic, is given by

$$Q_{2A}(x) = Q_A\left(\frac{qx(x+1)}{x+q}\right)(x+q)^{2A} \tag{46}$$

where $Q_1(x) = x$. Models such as these are interesting in studies of the roots of partition functions [24,25], since the computation of large numbers of zeros for such parti-

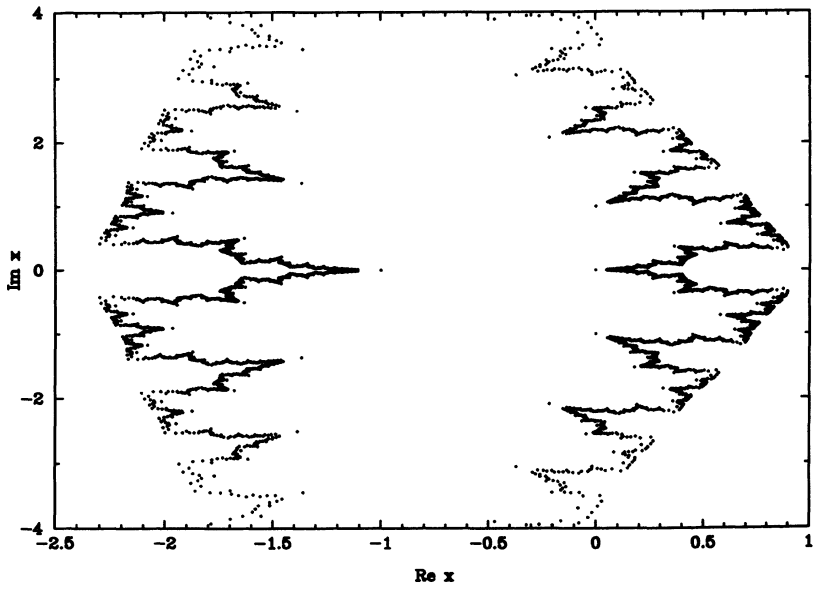

FIG. 2. Zeros of the partition function $Z_A(x)$ given by $Z_{2A}(x) = Z_A(-x(x+1)/(x-1))$, $Z_1(x) = x$, for $A = 4096$.

tion functions is easily accomplished. The distribution of roots in the complex plane can have a fractal character when the requirement that the coefficients be positive is relaxed. The case $q = -1$, shown in Fig. 2, reveals one such complex distribution of roots. In that case, the roots lie on the boundary of a series of copies of the Mandelbrot set. A discussion of zeros of the partition function for canonical models will be made in Sec. IV B.

IV. THERMODYNAMIC PROPERTIES OF FRAGMENTATION MODELS

In this section we consider the various thermodynamic functions that can be computed from the partition functions obtained from the weight given in Eq. (6). As an example, the specific heat for a finite Bose gas is computed. Finally, a discussion of phase transitions leads us to consider the location of the roots of the partition function on the complex plane for several models.

A. Thermodynamic functions

In Sec. II A we introduced a model with the thermodynamic variables confined to a single parameter x. Making this assumption allows us now to simply calculate the thermodynamic functions of such partition functions. Since

$$e^{-F(A,V,T)/k_BT} = A! \sum_{\mathbf{n}\in\Pi_A} \prod_{k=1}^{A} \frac{1}{n_k!} \left(\frac{x}{\beta_k}\right)^{n_k} \tag{47}$$

is the partition function for a thermodynamic system with $x = x(A,V,T)$, it is straightforward to calculate the thermodynamic functions from the free energy. First, let us introduce dimensionless variables for T and V

$$t \equiv \frac{T}{T_1}, \quad v \equiv \frac{V}{V_1} . \tag{48}$$

where T_1 and V_1 are arbitrary reference points, but convenient values for nuclear fragmentation are $k_BT_1 \equiv a_\nu$, $V_1 \equiv \frac{4}{3}\pi r_0^3 A$, where a_ν is defined in Sec. II A and r_0 is the classical radius of a nucleon.

We can express the various thermodynamic functions in terms of $\langle m\rangle$, $\langle m^2\rangle$, x, and its derivatives. The calculations are simple, and here we quote the results for the dimensionless pressure, energy, and specific heat:

$$p = PV_1/k_BT_1 = \langle m\rangle \left(\frac{t}{x}\frac{\partial x}{\partial v}\right) , \tag{49}$$

$$u = U/k_BT_1 = \langle m\rangle \left(\frac{t^2}{x}\frac{\partial x}{\partial t}\right) , \tag{50}$$

$$c_V = C_V/k_B = \langle m\rangle \left(2\frac{t}{x}\frac{\partial x}{\partial t} - \left(\frac{t}{x}\frac{\partial x}{\partial t}\right)^2 + \frac{t^2}{x}\frac{\partial^2 x}{\partial t^2}\right) + \left(\langle m^2\rangle - \langle m\rangle^2\right)\left(\frac{t}{x}\frac{\partial x}{\partial t}\right)^2 \tag{51}$$

where the ensemble averages of $m = \sum_k n_k$ are given by

$$\langle m\rangle = \frac{x}{Q_A(x)}\frac{\partial Q_A}{\partial x} ,$$
$$\langle m(m-1)\rangle = \frac{x^2}{Q_A(x)}\frac{\partial^2 Q_A}{\partial x^2} . \tag{52}$$

As an example, we can apply the above expressions to obtain the specific heat of a finite Bose gas. A Bose gas in d dimensions can be modeled by the x model, as noted in Sec. II A. Combining Eqs. (21), and (51) we arrive at a simple formula for the specific heat:

$$c_V = \frac{d}{2}\langle m\rangle + \frac{d^2}{4}(\langle m^2\rangle - \langle m\rangle^2) \tag{53}$$

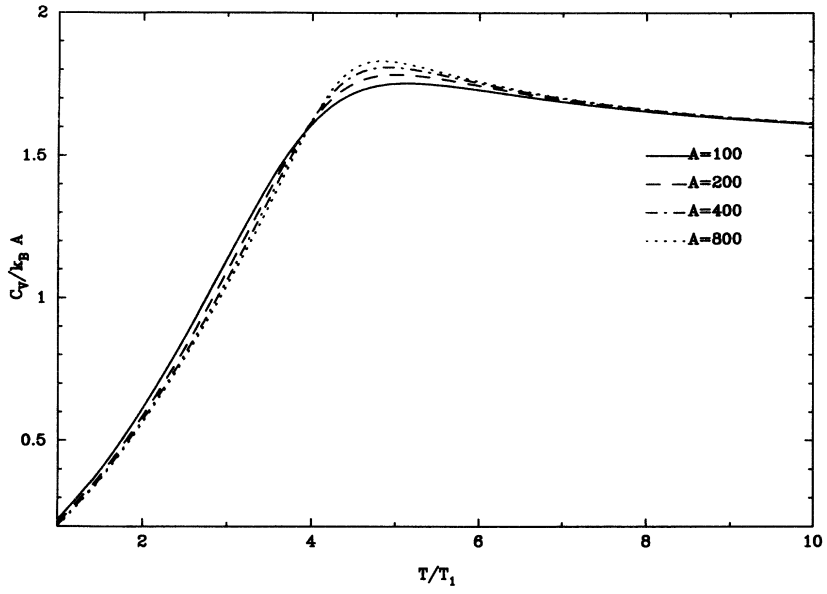

FIG. 3. Specific heat of a finite Bose gas for $d = 3$, $A = 100, 200, 400, 800$. $k_B T_1 = 8$ MeV in this figure.

assuming $x \propto T^{d/2}$. For $d > 2$, there is a phase transition (Bose-Einstein condensation) in the infinite particle limit, which can be seen as a cusp in the specific heat at the critical point, $x_c = A/\zeta(d/2)$. For finite gases, the partition function is smooth, so there is no cusp. However, the specific heat does reach a maximum near the critical point, suggesting the cusp will onset in the large particle limit. This behavior is illustrated in Fig. 3.

In the following subsection, we will consider another way of obtaining the phase transitions of a partition function. Using the results obtained in earlier sections, we attempt to calculate the zeros of the partition function for various A.

B. Zeros of the partition function and phase transitions

The canonical partition function $Z_A(x)$ is a polynomial of order A in x with positive coefficients. For example, for $\beta_k = k$, $Z_A(x) = x(x+1)\cdots(x+A-1)/A!$. By a theorem of Gauss, a polynomial of order A has A roots or zeros in the complex plane. For positive coefficients, no real roots are on the positive real axis, which is also the physical meaningful axis. The above example has its roots at the $x = 0$ and the negative integers $x = -1, -2, \ldots, -A+1$.

Complex roots correspond to an extension of the real temperature into the complex plane. Lee and Yang, in their discussion of phase transitions, showed that such transitions manifest themselves as zeros of the partition function approach the real positive axis as the thermodynamic limit $A \to \infty$ is approached. Taking the logarithm of the partition function to obtain the free energy can then lead to a singularity.

To illustrate the above remarks, we consider the example of the 2D Ising model on an $m \times n$ lattice. Kauffman [26] showed that the partition function for this model is given by

$$Z_{mn} = \prod_{r=1}^{m} \prod_{s=1}^{n} \left\{ \left(\frac{1+v^2}{1-v^2} \right)^2 - \frac{2v f_{rs}}{1-v^2} \right\} \tag{54}$$

where $f_{rs} = \cos(2\pi r/m) + \cos(2\pi s/n)$, $v = \tanh(J/k_B T)$. In this case the zeros of the partition function are located on two circles in the complex v plane, namely $v = \pm 1 + \sqrt{2}e^{i\theta}$. The physically meaningful domain of the v plane is the part of the real line $v \in (0, 1)$ (assuming $J > 0$). The zeros of the partition function approach this domain at one point, $v = -1 + \sqrt{2}$. This implies there should be a phase transition when

$$k_B T_c = \frac{J}{\tanh^{-1}(-1+\sqrt{2})} = \frac{2J}{\ln(1+\sqrt{2})} \tag{55}$$

which is the commonly known value for the critical temperature.

Now consider the zeros of the x model partition function in the complex x plane. The physically meaningful domain of x, the part with positive temperature, is the positive real axis. So for a phase transition to manifest itself in the infinite particle limit, the zeros of the partition function must approach the positive real axis. The $\beta_k = k$ model therefore has no phase transition, for in the infinite particle limit, the roots of the partition function are zero and the negative integers, which never approach the real temperature domain. Another example we consider is $\beta_k = k^\tau$ for the cases $\tau = 2, 3$. This corresponds to an ideal Bose gas in two and four dimensions by Eq. (21). So we expect that the zeros should approach the physically meaningful domain for large A for the case $\tau = 3$, but not for the case $\tau = 2$. Figure 4 illustrates the zeros for the models $\beta_k = k^2$ and $\beta_k = k^3$ for $A = 25, 50, 75, 100$. These graphs suggest that for both models, the roots lie on simple curves. Whether these curves close on the positive real axis is not clear from these small A results. The roots near the negative real axis scale with A, which suggests that the crossing

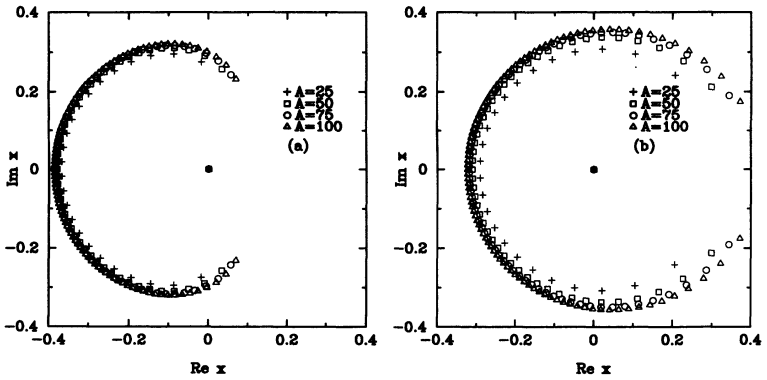

FIG. 4. Zeros of the partition function $Z_A(x)$ for the choice (a) $\beta_k = k^2$ and (b) $\beta_k = k^3$ scaled by $1/A$ (i.e., root x is plotted at x/A). The cases $A = 25, 50, 75, 100$ are shown.

point on the positive real axis should scale with A as well. This agrees with the known behavior of the critical point, which is given by $x_c/A = 1/\zeta(d/2)$. The fact that the curve will not close for $d = 2$ is not evident from the graph, however.

V. GENERAL BEHAVIOR OF MODELS AND COMPARISON WITH EXPERIMENTAL DATA

In this section we consider the general behavior of $\langle n_k \rangle$ for various β_k and how well these models proposed actually fit some experimental data obtained from heavy ion collider experiments [27]. These data were obtained from emulsion experiments for $^{197}_{79}$Au at 0.99 GeV/nucleon. 415 events were recorded and identified by the charges of the fragments, i.e. each event is represented by $\mathbf{n} = (n_1, \ldots, n_{79})$, where n_z represents the number of fragments with charge z in a given event. Ensemble averages were obtained by averaging over all events.

Since the experimental method only measured the electric charge of fragments leaving the collision, there is some question about how applicable are models developed considering only nucleons with no separation into protons and neutrons. Since the nuclear force treats protons and neutrons nearly identically, and the models proposed derived from a combinatorial viewpoint, the models should be identical whether one includes the neutrons or not. In fact, it can be shown that for the simple $\beta_k = k$ model, that the results are the same whether one considers Z nucleons coming out, or whether one considers A nucleons coming out, but only the Z protons can be followed, such that one must sum over the possible neutron configurations to obtain the expectation values.

A. General behavior of the models

Because all the models must satisfy $\sum_k k n_k = A$, there are restrictions on the form of the distribution. If we graph $\langle m_k \rangle = k\langle n_k \rangle$ vs k, then the area under the curve must be equal to A. For different choices of x and β_k, the area will be distributed differently. In this subsection we discuss typical distributions for these models.

All x models have simple behaviors at large and small x which are easy to obtain. For small x, all models will produce $\langle m_k \rangle$ with most of the area under $\langle m_A \rangle$. This is because for small x, the partition function is given almost entirely by the term proportional to x. This implies that one fragment is the most likely outcome. For $k \neq A$, $\langle n_k \rangle$ and $\langle m_k \rangle$ are proportional to x since

$$\langle n_k \rangle = \frac{x}{\beta_k} \frac{Z_{A-k}(x)}{Z_A} \approx x \frac{\beta_A}{\beta_k \beta_{A-k}} . \tag{56}$$

For large x, all models will produce $\langle m_k \rangle$ with most of the area under $\langle m_1 \rangle$. This is because for large x, the partition function is given almost entirely by the term proportional to x^A. So A fragments is the most likely outcome. For $k \neq 1$, $\langle n_k \rangle$ and $\langle m_k \rangle$ are proportional to x^{1-k} since

$$\langle n_k \rangle = \frac{x}{\beta_k} \frac{Z_{A-k}(x)}{Z_A} \approx \frac{x^{1-k}}{\beta_k} \frac{A!}{(A-k)!} . \tag{57}$$

The model $\beta_k = k$ was discussed in an earlier set of papers. For small x, most of the area is near $k = A$, as expected. For $x < 1$, $\langle m_k \rangle$ is monotonically increasing. At $x = 1$, $\langle m_k \rangle = 1$ for all k. For $x > 1$, $\langle m_k \rangle$ is monotonically decreasing. At large x, most of the area is near $k = 1$, as expected. This is shown in Fig. 5(a).

For models with $\beta_k = 1$, for $x \ll 1$ most of the area is below $k = A$. As x increases, some area is distributed along the rest of the graph, mostly around $k = A/2$. As x keeps increasing, the area continues to be redistributed, until most of it is distributed about a point $k < A/2$. At large x it takes on the usual distribution. This is illustrated in Fig. 5(b).

For the model $\beta_k = k^\tau$, with $0 < \tau < 1$, the behavior is very similar to $\beta_k = 1$. For small x, $\langle m_k \rangle$ increases monotonically, with most of the area near $k = A$. As x increases, the right-hand side is diminished till the graph attains two turning points, a local minimum near $k = A$, and a local maximum at a point $k < A/2$. The local minimum soon disappears, and the local maximum migrates left till it reaches $k = 1$ at large x. This behavior is illustrated in Fig. 5(c).

The models $\beta_k = k^\tau$, $\tau > 1$ are all very similar. For small x, $\langle m_k \rangle$ starts monotonically decreasing, reaches a minimum, then near $k = A$ rises rapidly. As x is in-

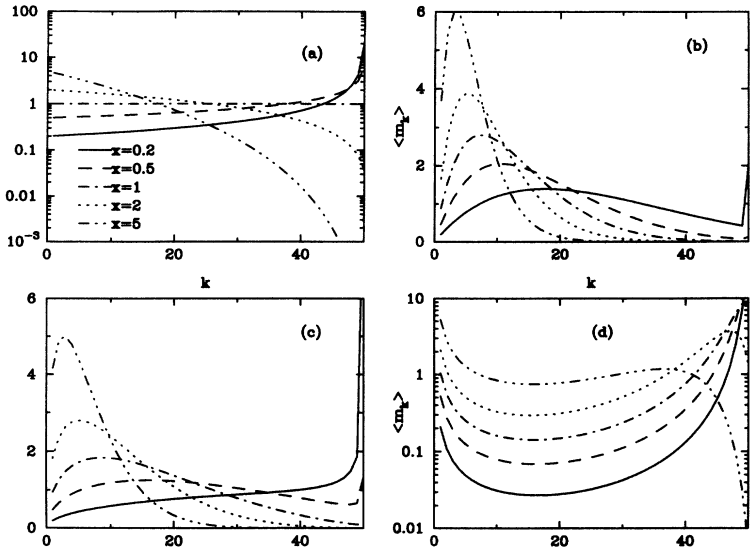

FIG. 5. The behavior of $\langle m_k \rangle$ vs k for $A = 50$, $x = 0.2, 0.5, 1, 2, 5$, $\beta_k = k^\tau$, where (a) $\tau = 1$, (b) $\tau = 0$, (c) $\tau = 1/2$, and (d) $\tau = 2$.

creased, the small k behavior is unchanged, but eventually the large k part turns downward. Thus for a small range of x, the graphs have two turning points. As x continues to increase, the local maximum eventually disappears and the typical large x behavior onsets. This behavior is shown in Fig. 5(d).

The model $\beta_k = k!$, for $x \ll 1$, $\langle m_k \rangle$ is mostly under $k = A$, as expected. From Eq. (56), we see $\langle n_k \rangle \approx x\binom{A}{k}$ for $k \neq A$, so the remainder of the area is binomially distributed about $k = A/2$. As x increases, the amount of area under $k = A$ diminishes, the balance appearing around $k \approx A/2$ in a binomial or Gaussian distribution. Once most of the area has disappeared from $k = A$, the Gaussian distribution at the center moves to the left as x is increased. For very large x, most of the area is under $k = 1$, as expected.

A simplified description of the $\beta_k = k!$ model can be obtained by making the following approximations. For a given x, the partition function is strongly peaked about a particular number of fragments $m = m_0$, such that $Q_A(x) \approx \mathcal{S}_A^{(m_0)} x^{m_0}$. To estimate m_0, we use the approximation for the Stirling numbers of the second kind, $\mathcal{S}_A^{(m)} \approx m^A/m!$, and maximize $Q_A(x)$. This gives a nonlinear equation for m_0, namely $m_0 = xe^{A/m_0} = m_0(A, x)$, where we have used Stirling's approximation for $m!$. We can then approximate $\langle n_k \rangle \approx \binom{A}{k} m_k^{-k} f_A(x)$ where $m_k = m_0(A - k, x)$ and $f_A(x)$ is a normalizing constant. We now make the assumption that $m_k \approx m_0(A - \langle k \rangle, x) \equiv \bar{m}$. The value of $f_A(x)$ can now be obtained by imposing the constraint $\sum_k k\langle n_k \rangle = A$, which gives

$$\langle n_k \rangle \approx \binom{A}{k} p^{k-1}(1-p)^{A-k} \tag{58}$$

where $p = 1/(\bar{m}+1)$. This distribution is binomial, with

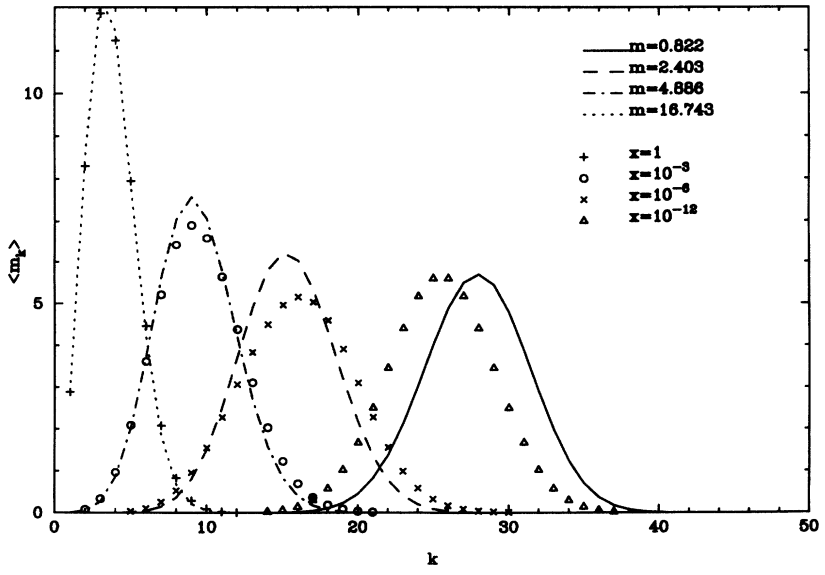

FIG. 6. The behavior of $\langle m_k \rangle$ vs k for $A = 50$, $\beta_k = k!$, at various x, with a comparison to the approximate model considered in the text. The lines correspond to the approximate model, the points to the exact model.

$\langle k \rangle = pA$. Using this result we arrive at an equation for $\bar{m}$,

$$\bar{m} = xe^{A/(\bar{m}+1)} . \tag{59}$$

Figure 6 compares the exact behavior with this approximation. From the figure we see that $\langle n_k \rangle$ is reasonably well described by this approximation.

B. Experimental comparisons

Nuclear fragmentation has a characteristic distribution which is met generically by only a few of the above models. For the experiment we will analyze, $\langle m_k \rangle$ drops, then rises. This suggests models with $\beta_k = k^\tau$ with $\tau > 1$ might be satisfactory if one x is used. Models with two or more x's are considered in Ref. [3]. The large k behavior is somewhat indeterminate. It could be rising or falling; there are not enough events to determine the behavior accurately.

Fits were made to $\ln\langle n_k \rangle$, dropping from the experimental distribution any $\langle n_k \rangle$ that were zero due to insufficient statistics. A previous paper [3] showed that for $x = 0.3$, the $\beta_k = k$ model gives a fairly good fit. A better fit is obtained by using two or more x's. Here, we consider the models which parallel models in other areas of physics. Specifically, $\beta_k = k^\tau$ is considered in analogy with the Bose gas in $d = 2(\tau - 1)$ dimensions as well as in analogy with various Markov process models. Also, $1/\beta_k = a/k + (1-a)/k^\tau$, with various τ is considered in analogy with Feynman's model for the λ transition in liquid helium [21]. The results are shown in Table IV, and in Fig. 7. For some choice of τ, x, and a, each of these models produced reasonable fits of the data, and appear to be better than the simple $\beta_k = k$ model.

TABLE IV. Fits of experimental data to various models.

β_k	x	a	τ	σ^2
k	0.296	n/a	n/a	78.58
k^τ	1.895	n/a	1.817	63.10
$\frac{k}{a+(1-a)k^{1-\tau}}$	0.93745	0	1.5	65.61
$\frac{k}{a+(1-a)k^{1-\tau}}$	1.96263	0.0587	2	62.34
$\frac{k}{a+(1-a)k^{1-\tau}}$	2.61313	0.0747	2.5	61.55
$\frac{k}{a+(1-a)k^{1-\tau}}$	3.0803	0.0732	3	62.20

VI. CONCLUSIONS AND SUMMARY

This paper presents a detailed investigation of a set of exactly solvable canonical ensemble models of fragmentation processes and discusses some of its parallels with other areas. Specifically, parallels between the description of the fragmentation process and other areas are developed which include Feynman's approach to the λ transition in liquid helium, Bose condensation, and Markov process models.

The partition functions derived from various weights given to each member of the canonical ensemble, are shown to be polynomials in a parameter x. Simple recurrence procedures are developed for obtaining the partition function and the coefficients in the associated polynomials. The variable x, called a tuning parameter, contains the underlying physical quantities associated with the description of the the different processes considered. For example, in nuclear fragmentation, x involves the thermodynamic variables V (volume) and T (temperature) through the quantum volume $v_0(T)$ as well as binding energy and excitation energy coefficients.

Besides the tuning parameter x, the weight given to each member of the ensemble contains a quantity β_k which gives the cluster size dependence of this weight. Various choices for β_k are considered, and a wide range

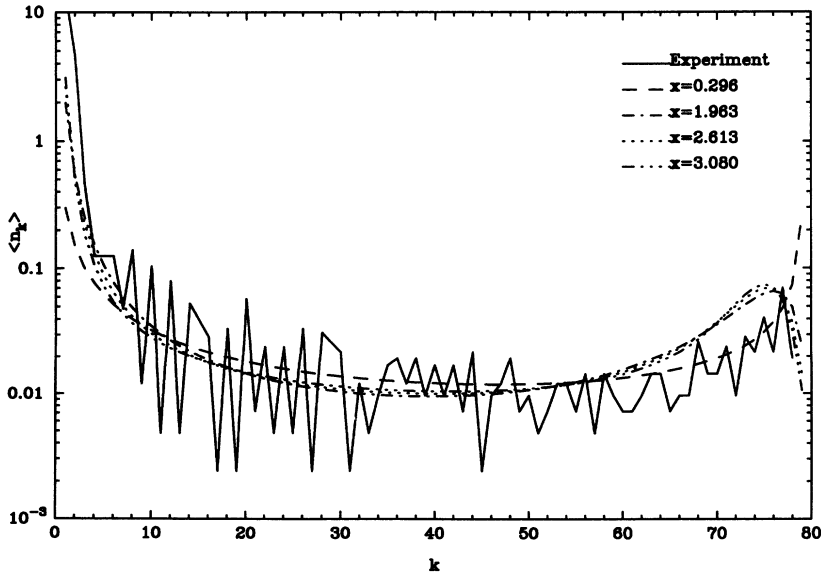

FIG. 7. $\langle n_k \rangle$ vs k for various x and β_k. Line $x = 0.296$ has $\beta_k = k$. Line $x = 1.963$ has $\beta_k^{-1} = a/k + (1-a)/k^2$. Line $x = 2.613$ has $\beta_k^{-1} = a/k + (1-a)/k^{5/2}$. Line $x = 3.080$ has $\beta_k^{-1} = a/k + (1-a)/k^3$.

of different types of behavior can be found for different choices for β_k. A previous model of fragmentation [1–3] used $\beta_k = k$, a choice leading to very simple results. The more general form, $\beta_k = k^\tau$, is investigated here. Also considered here is the choice $\beta_k = k!$. The expected distribution of fragments for this choice is a number of fragments all of nearly equal size.

The canonical models presented in this paper can all be derived from Markov processes. Markov process models can give a picture of the underlying physical processes that lead to cluster formation and break up. The relationship of this approach to that based on the canonical ensemble is discussed.

A consideration of the thermodynamics of fragmentation systems led to an investigation of the behavior of the partition function when x is a complex number. In particular, the zeros of the partition function are studied in the complex plane and the connection with the Lee-Yang theorems and phase transitions are investigated for various choices of β_k. More complex iterative models of the partition function are proposed whose distribution of zeros can be fractal sets.

Finally, some experimental data are investigated. Various choices for the quantity β_k are considered in our analysis. The statistics of the data are not sufficient to distinguish the various possible β_k's considered, however the results of these more general models appear to be better than the earlier model $\beta_k = k$.

ACKNOWLEDGMENTS

This work was supported in part by the National Science Foundation Grant No. NSFPHY 92-12016.

[1] A. Z. Mekjian, Phys. Rev. Lett. **64**, 2125 (1990); Phys. Rev. C **41**, 2103 (1990).
[2] A. Z. Mekjian and S. J. Lee, Phys. Rev. A **44**, 6294 (1991).
[3] S. J. Lee and A. Z. Mekjian, Phys. Lett. A **149**, 7 (1990); Phys. Rev. C **45**, 365 (1992); **45**, 1284 (1992).
[4] S. Sobotka and L. Moretto, Phys. Rev. C **31**, 668 (1985).
[5] J. Aichelin and J. Hufner, Phys. Lett. **136B**, 15 (1984).
[6] X. Canupi, J. Phys. A **19**, L917 (1986); Phys. Lett. B **208**, 351 (1988).
[7] J. Desbois, Nucl. Phys. **A466**, 724 (1987).
[8] H. R. Jaqaman, A. R. DeAngelis, A. Ecker, and D. H. E. Gross, Nucl. Phys. **A541**, 492 (1992).
[9] H. R. Jaqaman and D. H. E. Gross, Nucl. Phys. **A524**, 321 (1991).
[10] A. R. DeAngelis and A. Z. Mekjian, Phys. Rev. C **40**, 105 (1989).
[11] A. R. DeAngelis, D. H. E. Gross, and R. Heck, Nucl. Phys. **A537**, 606 (1992).
[12] D. H. E. Gross, A. Ecker, and A. R. DeAngelis, Ann. Phys. (Leipzig) **1**, 340 (1992).
[13] D. H. E. Gross, L. Sapathy, M. Ta-Chung, and M. Sapathy, Z. Phys. A **309**, 41 (1982); D. H. E. Gross and X. Zhang, Phys. Lett. **161B**, 47 (1985).
[14] S. Koonin and J. Randrup, Nucl. Phys. **A474**, 173 (1987).
[15] L. P. Csernai and J. Kapusta, Phys. Rep. **131**, 223 (1986).
[16] D. H. Boal and J. N. Glosi, Phys. Rev. C **38**, 1870 (1988).
[17] A. J. Cole, Phys. Rev. C **40**, 2024 (1989).
[18] C. Fai and J. Randrup, Nucl. Phys. **A404**, 551 (1983).
[19] W. A. Friedman, Phys. Rev. C **42**, 667 (1990).
[20] J. Bondorf, R. Donagelo, I. N. Mishustin, and H. Schule, Nucl. Phys. **A444**, 460 (1985).
[21] R. P. Feynman, *Statistical Mechanics: A Set of Lectures, Frontiers in Physics* (Benjamin/Cummings, Reading, MA, 1972).
[22] F. P. Kelly, *Reversability and Stochastic Networks* (Wiley, New York, 1979).
[23] *Handbook of Mathematical Functions*, edited by M. Abramowitz and I. Stegun, Natl. Bur. Stand. Appl. Math. Ser. No. 55 (U.S. GPO, Washington, D.C., 1965).
[24] B. Derrida, L. DeSeze, and C. Itzykson, J. Stat. Phys. **44**, 559 (1983).
[25] H. O. Peitgen and P. H. Richter, *Proceedings of the International School of Physics "Enrico Fermi,"* Course IC, edited by G. Cagiotti, H. Haken, and L. Lugiato (North-Holland, Amsterdam, 1988).
[26] B. Kauffman, Phys. Rev. **76**, 1232 (1949).
[27] C. J. Waddington and P.S. Freier, Phys. Rev. C **31**, 88 (1985).